International Journal of General Medicine

Dovepress
Taylor & Francis Group

Open Access Full Text Article

ORIGINAL RESEARCH

Whole-Genome Methylation Sequencing Analysis and Functional Verification of LIM-Homeobox Family Genes in Cervical Cancer

Rong Yu[1,*], Qin Yu[1,*], Jie Shi[2,*], Xue Meng[3], Zhiyuan Deng[3], Jing Suo[4], Hao Yang[1]

[1]Department of Radiation Oncology, Peking University Cancer Hospital (Inner Mongolia Campus) & Affiliated Cancer Hospital of Inner Mongolia Medical University, Huhhot, Inner Mongolia Autonomous Region, 010020, People's Republic of China; [2]Department of Gynecology and Oncology, Peking University Cancer Hospital (Inner Mongolia Campus) & Affiliated Cancer Hospital of Inner Mongolia Medical University, Huhhot, Inner Mongolia Autonomous Region, 010020, People's Republic of China; [3]Department of Graduate School, Inner Mongolia Medical University, Hohhot, Inner Mongolia Autonomous Region, 010059, People's Republic of China; [4]Department of Gynecology and Obstetrics, the Affiliated Hospital of Inner Mongolia Medical University, Hohhot, Inner Mongolia Autonomous Region, 010050, China

*These authors contributed equally to this work

Correspondence: Hao Yang, Department of Radiation Oncology, Peking University Cancer Hospital (Inner Mongolia Campus) & Affiliated Cancer Hospital of Inner Mongolia Medical University, No. 42, Zhao Wu Da Road, Huhhot, Inner Mongolia Autonomous Region, 010020, People's Republic of China, Tel +86 471-3280801, Email hdgeu98@163.com; Jing Suo, Department of Gynecology and Oncology, Affiliated People's Hospital of Inner Mongolia Medical University, 1 Tongdao North Street, Hohhot, Inner Mongolia Autonomous Region, 010050, People's Republic of China, Tel +86 471-3451350, Email suojing49@sina.com

Background: Gene methylation in cells is an important factor in tumorigenesis, and radiotherapy can change DNA methylation in cells. In this study, complete genome methylation sequencing (BS-Seq) technology was used to analyze the genome-wide methylation of patients with cervical cancer before and after radiotherapy.

Methods: Three pairs of cervical squamous cell carcinoma samples were collected from patients before and after radiotherapy in July 2020. Genome-wide DNA methylation profiles were generated using WGBS. Bioinformatics analysis was conducted to identify differential methylation regions (DMRs) and their associated genes and pathways. The study focused on the methylation changes of LHX2, LHX5, and LHX9 genes, assessing their expression levels using qRT-PCR and correlating these changes with cervical cancer stages.

Results: MCG was the main way of genomic DNA methylation in the three patients. The DNA methylation level and methylation density on each chromosome varied greatly. As revealed by comparison of methylation before and after radiation in the three patients, 1287, 1261 and 789 differential methylation genes were identified, respectively. 3) Combined with clinical treatment, methylation level difference and correlation enrichment analysis, it was found that LHX2, LHX5 and LHX9 were closely related to the occurrence and development of cervical cancer. After 5-Aza-DC and radiotherapy, the methylation of the CpG islands in LHX2, LHX5 and LHX9 genes in these patients was decreased ($p < 0.01$), and the mRNA and protein expression levels were relatively increased ($p < 0.01$).

Conclusion: In our present work, genome-wide DNA methylation maps of cervical cancer tissues before and after radiotherapy were successfully constructed. We found that LHX5 and LHX9 genes are closely related to cervical cancer. LHX5 and LHX9 have a negative effect on cervical cancer. The migration ability of LHX9 silenced cells was significantly enhanced after irradiation.

Keywords: cervical cancer, radiation therapy, whole-genome bisulfite sequencing, WGBS, LHX2, LHX5, LHX9

Background

Cervical cancer is one of the most prevalent cancers among women, affecting approximately 500,000 individuals globally each year. In 2008, there were about 529,800 new cases of cervical cancer and 255,100 related deaths worldwide, with 85% of these cases occurring in developing countries.[1] Squamous cell carcinoma is the most common pathological type of cervical cancer, followed by adenocarcinoma. Notably, the incidence of cervical cancer has been increasing among younger women.[2]

Received: 27 April 2024
Accepted: 8 December 2024
Published: 8 January 2025

DNA methylation, a widespread epigenetic modification in eukaryotic cells, involves the addition of a methyl group to DNA, typically at CpG dinucleotide sites. This process is mediated by DNA methyltransferases (DNMTs) and uses S-adenosyl methionine (SAM) as the methyl donor.[3,4] In mammals, DNA methylation predominantly occurs at CpG sites and plays a crucial role in genome-wide and local gene regulation. It is involved in a variety of biological processes, including the spatiotemporal expression of genes, X chromosome inactivation, aging, cancer development, and species evolution.[5]

Whole-genome bisulfite sequencing (WGBS) is a powerful technique for analyzing DNA methylation across the entire genome. By combining bisulfite treatment with high-throughput DNA sequencing, WGBS provides single-base resolution of methylation patterns, allowing for precise measurement of methylation levels.[6] This technique has been applied to various clinical studies, including those on lung[7] and gastric cancers.[8] In 2020, Li Meng et al explored the relationship between DNA methylation in the ZNF772 promoter and its expression in cervical cancer.[9]

Several genome-wide methylation sequencing methods are available, including bisulfite sequencing (BS-Seq), methylated DNA immunoprecipitation (MeDIP-Seq), and methylated DNA enrichment coupled with high-throughput sequencing (MBD-Seq). Among these, BS-Seq is considered the gold standard for detecting methylation levels due to its comprehensive coverage of both common and specific methylation sites. Integrating these methods with high-throughput sequencing enhances the coverage and detail of DNA methylation maps. For example, BS-Seq was used to construct the DNA methylation map of Jinghai yellow chicken thigh muscle, identifying IGF2BPL and IGF2BP3 as growth-related genes.[10]

Gene methylation is a critical factor in tumorigenesis, and radiotherapy is a common treatment modality that can alter DNA methylation levels in cancer cells. Studies in mice have shown that radiotherapy-induced methylation changes are dose-dependent.[11] Radiotherapy can downregulate key methylation enzymes, such as DNMT1, DNMT3A, and DNMT3B, leading to global demethylation and subsequent changes in gene expression, including the upregulation of tumor suppressor genes.[12,13] For instance, radiotherapy has been associated with reduced mutation rates in K-ras and MGMR genes in cancer tissues, highlighting its potential for tumor control and surgical outcomes.[13] Furthermore, changes in methylation states can affect radiosensitivity in a gene-specific manner, with hypermethylation of certain genes (eg, Axin, ATM, MGMT, TIMP3) or hypomethylation of others (eg, SerpinB5, S100A6) influencing cancer cell response to radiation.[14]

Based on these findings, we hypothesize that radiotherapy induces specific alterations in DNA methylation, which in turn regulate the expression of genes involved in tumor suppression and progression. Additionally, HPV vaccination has emerged as a crucial factor in cervical cancer prevention and prognosis. The vaccine targets the human papillomavirus, the primary cause of cervical cancer, significantly reducing the incidence of cervical intraepithelial neoplasia (CIN) and cervical cancer. Recent studies suggest that DNA methylation may also influence the effectiveness of HPV vaccination, as methylation of viral and host genes can affect viral persistence and oncogenesis. For example, methylation of the HPV16 L1 gene has been linked to viral clearance, indicating that methylation status could impact vaccine efficacy.[15,]

In this study, we utilized next-generation sequencing technology to perform WGBS on cervical cancer tissues before and after radiotherapy. By mapping methylation dynamics, we aimed to identify key genes involved in cervical cancer progression and radiotherapy sensitivity, providing a theoretical foundation for understanding the pathogenesis and treatment of cervical cancer.

Materials and Methods

Clinical Samples and Cells

According to the clinical diagnosis results, we selected 3 patients with cervical squamous cell carcinoma (D, M and W) in July 2020. Inclusion Criteria: All participants must have a confirmed pathological diagnosis of cervical squamous cell carcinoma. Participants must be candidates for radiotherapy, specifically those diagnosed at an early stage and scheduled for radiation treatment. All patients must receive a standard radiotherapy protocol to ensure consistency and comparability of data. Participants must be between 18 and 65 years old to exclude the different physiological conditions of children and elderly patients. All participants must sign an informed consent form, acknowledging their understanding and agreement to participate in the study. Exclusion Criteria: Other Malignancies: Participants with other types of malignant tumors are excluded. Severe Medical or Psychiatric Conditions: Participants with severe internal or psychiatric

diseases that could interfere with treatment or follow-up are excluded. Pregnancy or Lactation: Pregnant or breastfeeding women are excluded from the study. The samples were collected before and after radiotherapy. Cervical cancer Siha and C33A cells were provided by ATCC cell bank (USA).

DNA Extraction

DNA was extracted with TIANamp Genomic DNA Kit (Tiangen, China) with the specific instruction. DNA quality was assessed using a NanoDrop spectrophotometer and an Agilent 2100 Bioanalyzer.

Bisulfite Sequencing Experiment and Sequencing

Prior to bisulfite administration, we introduced 25 ng lambda-DNA in 5 ug genomic DNA obtained from cervical cancer. Then, the Sonicator (Sonics & Materials) was utilized to fragment the DNA mixture to 300bp. Following blunt ending and dA 3'-end addition, we cloned Illumina methylated adapters in line with specific protocols. Later, M. anisopliae DNA was converted with bisulfite with ZYMO EZ DNA Methylation-Gold kit (ZYMO), followed by amplification through 12 PCR cycles. Illumina HiSeq 2500 was utilized for ultra-high-throughput pair-end sequencing in line with specific protocols. Meanwhile, Illumina base-calling pipeline (SolexaPipeline-1.0) was adopted for processing raw HiSeq sequencing data.

Following the delivery of DNAs, the sample quality test was carried out. Thereafter, qualified DNAs were adopted for constructing the BS library, and its quality was also tested. Finally, the qualified BS library was applied in sequencing by Illumina NovaSeq 6000 sequencing (150bp*2, Shanghai BIOZERON Co., Ltd.).

Reads Quality Control

Through using Trimmomatic with parameters (SLIDINGWINDOW:4:15 minLEN:75) (version 0.36 http://www.usadellab.org/cms/uploads/supplementary/Trimmomatic), trimming and quality control of raw paired end reads were completed.

Mapping Sequence Data to Reference

We mapped the clean reads to the reference genome using the BSMAP aligner and allowed 2 mismatches (Xi and Li, 2009 BSMAP: whole-genome bisulfite sequence MAPping program). Later, cytosine methylation state was determined based on uniquely mapped reads according to a previous description (Lister et al, 2008 highly integrated single-base resolution maps of the epigenome in Arabidopsis).

Methylation Level Stat

Use in House Perl Script to Do Basic Methylation Level Stat

Identification of Differential Methylation Regions (DMRs)

For identifying DMRs, just cytosines covered by 4 or more reads within one library were taken into consideration. The 200bp sliding-window was utilized to search DMRs, and the step-size was set at 50bp. We later conducted Fisher's exact test to compare DNA methylation states in diverse plants and adjusted p-values for multiple comparisons by Benjamini–Hochberg approach. We retained windows whose FDR < 0.05 and fold change >1.5 in methylation level in later analyses. Additionally, p-value for every cytosine within a selected region was determined through Fisher's exact test, with p <= 0.01 and FC >= 2 being the thresholds to identify differentially methylated cytosine (DMC). The absolute methylation differences of CG, CHG and CHH were 0.4, 0.2, and 0.1 separately. Only regions containing 7 or more DMCs were kept. Finally, we integrated adjacent DMRs when the gap was <= 100bp (Lister et al, 2009 human DNA methylomes at base resolution show widespread epigenomic differences).

DMR Annotation

Use in House Perl Script to Do DMR Annotation

DMR Overlap Gene Functional Enrichment

For understanding functions of DMR overlap genes, we conducted GO and KEGG analyses with Goatools (https://github.com/tanghaibao/Goatools) and KOBAS (http://kobas.cbi.pku.edu.cn/home.do). The significant enrichment of DEGs into GO terms and metabolic pathways was determined at Bonferroni-corrected P < 0.05.

Data Visualization

We visualized genome-wide expression and DNA methylation levels using either Integrative Genomics Viewer (IGV) (Thorvaldsdóttir et al, 2013 Integrative Genomics Viewer) or Integrated Genome Browser (IGB) (Nicol et al, 2009).

Bsp Pcr

Methyl primer express v1.0 was utilized to design BSP primers. The PCR reactions were carried out within the 50-μL system containing 10x PCR Buffer (Mg++, 8 μL); dNTP mixture (2.5 mm each, 4 μL); Taq polymerase (5U/L, 0.5 μL); respective primers (10 μM, 1 μL), and environmental DNA (5–10 ng, a template). The PCR process:5-min under 95 °C; 30-s under 94°C, 30-s under 56°C and 25-s under 72°C for 30 cycles; and 7-min under 72 °C. We delivered positive clones for sequencing in the biotech company. Methylation level in every sample was determined below:

$$\text{Methylation Level in Every Sample (\%)}=C/(*nc*n)100\%$$

Where C indicates the methylation site number within every sample; N indicates sample number; Nc represents cloning number; and n suggests CpG number.

Meanwhile, Methylation Rate in Every Sample Group Was Determined Below:

$$\text{Methylation Rate in Every Group (\%)}= \text{Methylation Rate in Every Sample of the Group}/N$$

RNA Extraction and the First-Strand cDNA Preparation

RNA was first isolated with Trizol reagent (Invitrogen, CA, USA) in line with specific protocols and later synthesized into first-strand cDNA using the transcriptor first-strand cDNA synthesis kit (Roche) in line with specific protocols.

Quantitative Real-Time PCR (qRT-PCR) Validation

Prime Primer 5 was utilized for primer design in Beijing Genomics Institute (Table 1). β-actin (ACT3) was used as the endogenous control. qRT-PCR was carried out with SYBR Green dye (LightCycle® 480 SYBR Green I master). Afterwards, LightCycle® 480 Real-Time PCR System was employed for verifying those chosen genes. The PCR process: 10-min under 95 °C; 10-s under 95°C, 30-s under 60°C and 20-s under 72°C for 40 cycles. Dissolution curve: 72°C~95°C, Heating Rate, 0.5°C/10s. Melting curve analysis was adopted to analyze the qPCR product specificity. In addition, gene expression was analyzed by 2-ΔΔCt approach.

Effects of Radiation on Cervical Cancer Cells

Radiation treatment of cells was performed. Briefly, cervical cancer cells (SiHA and C33A, 1×105) and HCerEpic cells were cultured within the culture flask. At 24-h after cell adherence, we carried out X-ray irradiation for 24 hours. Then,

Table 1 Prime Sequences for qRT-PCR

Primer name		Primer sequence (5'-3')
LHX2	F	GAGAGGAGGAGAACTGAG
LHX2	R	CTTCTGGGCCATCATCTCCT
LHX5	F	CACTCAGTTCAGCAGGGGTA
LHX5	R	TGACACAGTGGTCTCCCTTC
LHX9	F	GTCCAGTCAGTCAGGCTCTT
LHX9	R	ATTCGGTACACCTGGTAGAA
β-actin	F	GCCAAAAGGGTCATCATCTC
β-actin	R	GTAGAGGCAGGGATGATGTTTC

Note: HX2, LIM Homeobox 2; LHX2, LIM Homeobox 5; LHX9, LIM Homeobox 9; F, forward; R, Reversed.

2Gy X-ray irradiation was performed for 24 h. We removed the original culture medium at 48 h after radiation treatment, added trypsin for cell digestion, and harvested cells. After washing twice by PBS, cells were harvested. For confirming the effect of 6 MV X-ray on cells, this study used 2, 4, 6, 8 and 10 gy and so on five different doses of radiation processing cells, found that radiation after 24 hours, in addition to the 2 gy and 4 gy two doses of the cell morphology and the number is still in the high status, 6–10 gy ray entered the stage of apoptosis cells have a lot of processing, not normal for subsequent experiments. 2 gy was chosen as the experimental dose. Cell invasion and migration abilities were assessed by Transwell assay. RNA was extracted with Trizol reagent (Sigma, USA) with specific instruction.

Statistical Analysis

The data were presented as mean ± SEM, and statistical analyses were performed using GraphPad Prism 7.0 software (http://www.graphpad.com/scientific-software/prism). A one-way ANOVA/Two-way repeated ANOVA was employed to assess statistical significance, defined as $*p < 0.05$, $**p < 0.001$, and $***p < 0.0001$.

Results

Methylation Sequencing

In the present work, three cervical cancer tissues before and after radiotherapy were selected for BS-Seq analysis, and the original sequencing sequence data obtained, respectively, averaged 706630178 (Q20 > 96%, Supplementary Figure 1) . After quality control, clean reads were 602534129 (Q20 > 98%, Table 2), its quality distribution was shown in supplementary Figures 2 and 3. We utilized BSMAP software for determining unique read number and proportion to the human genome. Before radiotherapy, the mapping rates of D, M and W were 75.89%, 77.26% and 80.12%, respectively. After radiotherapy, the mapping rates of D, M and W were 74.98%, 74.89% and 75.83%, respectively. The average matching rate of three individuals before and after radiotherapy was 77.76% and 75.23% respectively. The proportion of bases with a sequencing depth of 5 × accounted for more than 83.71% of the total length of the genome, and the biological duplication was three.

Methylation Basic Information Statistics

Proportion Statistics of Different Types of Methylation Sites

Diverse methylated C sites occur under various sequence environments at varying proportions. The average number of mC increased by 79983691 after radiotherapy compared with before radiotherapy. Before radiotherapy, the average proportion of mCG, mCHG and mCHH sites was 83.55%, 3.59% and 12.86%, respectively (Supplementary Figure 2). After radiotherapy, the mCG, mCHG and mCHH loci averaged 80.58%, 4.91% and 17.17%, respectively. The proportion of mCG reduced by 2.96%, and the proportion of mCHG and mCHH increased by 1.31% and 4.28%, respectively.

Methylation Level Distribution in Functional Regions

For each context, C sites within diverse genomic functional regions, including gene, Promoter (prom), exon and down, etc. The prom region includes a 2-KB region in the site upstream. Before radiation, the proportions of mC, mCG, mCHG and mCHH within four functional regions (gene, prom, exon and down) were lower than after radiation (Supplementary

Table 2 Statistical Table of Original Sequencing Data

Sample_ID	Total_Reads	Total_Bases	GC%	Total_Reads	Clean reads	Mapped reads	Mapped rate
DB	722523242	108378486300	22.85	722523242	587051454	445533609	0.7589
DF	657269506	98590425900	22.90	657269506	563293398	422366107	0.7498
MB	659871314	98980697100	22.26	659871314	576978050	445760130	0.7726
MF	713362030	107004304500	22.51	713362030	620738000	464882611	0.7489
WB	773487294	116023094100	22.65	773487294	644536034	516389482	0.8012
WF	713267684	106990152600	22.27	713267684	622607836	472109898	0.7583

Abbreviations: DB, patient D before radiotherapy; DF, patient D after radiotherapy; MB, patient M before radiotherapy; MF, patient M after radiotherapy; WB, patient W before radiotherapy; WF, patient W after radiotherapy.

Figure 3). After radiation, mCG decreased by 0.13% in the prom region. The sequence environment methylation of mCG presented hypermethylation levels in four functional regions, and the methylation level is 58%-80%. The mean mCG methylation level within the prom region is 58.04%, and the hypermethylation level away from the 5 'end is increased.

Differentially Methylated regions (DMR) represent genomic regions showing significantly differential levels of methylation between diverse samples. These regions are crucial for regulating gene levels. DMR distribution on the genome can be diverse (promoters, exons, introns and intergene regions, etc.), so the ways of DMR regulating gene expression are also diverse. Based on genome-wide methylation analysis, there were 2666 differential methylation sites in patients before and after D radiation, among which 1856 sites had elevated methylation levels and 810 sites had significantly decreased methylation levels. There were 2873 differential methylation sites in patients with M before and after radiation, including 1,976 sites with significantly increased methylation level and 905 sites with significantly decreased methylation level. There were 1411 differential methylation sites in patient W before and after radiation, among which 300 sites had significantly increased methylation level and 1111 sites had significantly decreased methylation level. The DNA methylation level and methylation density on each chromosome varied greatly.

Tumor tissue samples from patients before and after radiotherapy were selected for sequencing, and it was found that D and M gene methylation levels of patients with effective treatment group (radiosensitive group) were similar. The LHX family gene showed significantly down-regulated methylation levels within cervical cancer tissues after treatment, with significant differences. Methylation changes in 2 effective patients were consistent (Table 3). The degree of difference in methylation level and the annotation results were combined, Hist1H3J showed a 12-fold decrease in D methylation, while MYC gene showed a 65-fold increase after radiotherapy in 3 patients. C10ORF11 was reduced in patients with W methylation with a 73-fold difference. Multiple members of the LHX family have hypomethylation after radiotherapy, and LHX2, LHX5, and LHX9 appear together in patients D and M who respond to radiotherapy. The changes of LHX2, LHX5 and LHX9 gene methylation in LHX family were not significant in patients who failed to receive radiotherapy.

Table 3 Changes of Methylation Levels of Some Key Genes in D, M and W Patients Before and After Radiotherapy

	Gene annotation	D			M		
		Before	After	Fold	Before	After	Fold
ENSG00000148655	C10orf11	0.23	0.86	3.7	0.31	0.94	3.1
ENSG00000156206	C15orf26	0.12	0.91	7.6	0.36	0.92	2.6
ENSG00000142609	C1orf222	0.35	0.75	2.1	0.62	0.11	5.4
ENSG00000188523	C9orf171				0.62	0.13	4.7
ENSG00000197153	HIST1H3J	0.78	0.06	12.6	0.12	0.64	5.5
ENSG00000132130	LHX1	-	-	-	0.55	0.04	12.6
ENSG00000106689	LHX2	0.63	0.13	4.8	0.34	0.16	2.1
ENSG00000089116	LHX5	0.41	0.06	6.5	0.50	0.03	14.5
ENSG00000106852	LHX6	-	-	-	-	-	-
ENSG00000162624	LHX8	-	-	-	-	-	-
ENSG00000143355	LHX9	0.66	0.12	5.4	0.27	0.11	2.4
ENSG00000136997	MYC	0.88	0.24	3.6	0.00	0.66	65.9
ENSG00000183780	SLC35F3	0.33	0.95	2.9	0.47	0.13	3.7
ENSG00000022567	SLC45A4	0.81	0.27	3.1	0.36	0.06	5.8
ENSG00000118160	SLC8A2	0.44	0.04	11.7	0.41	0.89	2.2

Abbreviations: C10orf11, Chromosome 10 Open Reading Frame 11; C15orf26, Chromosome 15 Open Reading Frame 26; C1orf222, Chromosome 1 Open Reading Frame 222; C9orf171, Chromosome 9 Open Reading Frame 171; HIST1H3J, Histone Cluster 1 h3 Family Member J; LHX1, LIM Homeobox 1; LHX2, LIM Homeobox 2; LHX5, LIM Homeobox 5; LHX6, LIM Homeobox 6; LHX8, LIM Homeobox 8; LHX9, LIM Homeobox 9; MYC, Myc Proto-Oncogene; BHLH, Transcription Factor; SLC35F3, Solute Carrier Family 35 Member F3; SLC45A4, Solute Carrier Family 45 Member A4; SLC8A2, Solute Carrier Family 8 Member A2.

GO Enrichment Analysis of Differential DMR Gene

When the region where differentially methylated genes overlap with functional parts of the genes in the specific region, we screened out the related genes, which were called the differentially methylated regions related genes, which directly reflected the number distribution of DMGS-related genes on the GO term where biological process (BP), cell component (CC) and molecular function (MF) were enriched. According to GO function enrichment analysis, 391, 78 and 120 differential functions were associated with BP, CC and MF in D patients before and after radiotherapy, respectively, with a total of 589 differential functions. In M patients, 540, 61 and 84 differential functions were enriched in BP, CC and MF categories, separately, with a total of 685 differential functions. In patient W, 555, 55 and 74 differential functions were enriched in BP, CC and MF, separately, with a total of 684 differential functions.

The GO function of the three groups, DB-DF-CG, MB-MF-CG and WB-WF-CG, was enriched, and the top 30 groups with significant differences were shown in Supplementary Figure 4. The results of GO enrichment showed that the growth, development, plasma membrane projections and membranous projections and anatomical structure development were significantly correlated with the results of GO enrichment. The accumulation degree of cell adhesion and other functions is high.

Table 4 Expression Levels and Methylation Levels in 47 Cervical Cancer Tissues

Number	Pathologic types	FIGO staging	LHX2		LHX5		LHX9	
			Gene expression	Promoter methylation level率	Gene expression	Promoter methylation level率	Gene expression	Promoter methylation level率
80032286	Squamous cell carcinomas	IVB	0.24	0.48	7000.12	0.12	2531.80	0.17
80034672	Squamous	IIIC1r	0.30	0.46	72.83	0.18	1950.14	0.19
80031441	Squamous	IIA	1.00	0.40	3.90	0.42	1.00	0.30
80028734			0.25	0.48	4.58	0.38	0.41	0.36
80035887	Squamous	IIIC1r	0.35	0.56	28.35	0.19	6331.96	0.12
80030752	Squamous	IIIC	0.20	0.45	33.86	0.19	490.43	0.16
80037001			2.26	0.31	30.60	0.19	0.08	0.32
80032006	Squamous	IIIC1r	0.20	0.46	110.00	0.15	1369.00	0.21
80028978	Squamous	IIB	1.00	0.39	5.51	0.36		
80029084	Squamous	IIA	0.80	0.42	2.09	0.41	0.34	0.35
80036657			0.40	0.52			0.29	0.39
80029531			1.75	0.36	1.75	0.44	5.28	0.27
80029869	Squamous	IIIB	0.43	0.53	181.86	0.11	109.55	0.13
80036518			0.28	0.43	0.00		0.00	0.38
80034921			0.15	0.45	0.00		0.00	0.39
80029647	Squamous	IIIC	0.29	0.43	223.75	0.11	505.87	0.14
80028814	Squamous	IIIB	1.00	0.44	146.00	0.12	198.00	0.23
80029418	Squamous	IIIC1r	4.49	0.21	864.99	0.09		
80033033	Squamous	IIIC1r	0.84	0.42	100.43	0.16	181.75	0.25
80036164	Squamous	IIB	0.93	0.40	9.61	0.28	18.37	0.24
80040252	Squamous	IIIC1r	1.00	0.40	169.00	0.13	1993.20	0.18
80040268	Squamous	IIB	1.97	0.33	44.44	0.15	104.40	0.26
80028084	Squamous	IIIC1r	0.46	0.51	68.14	0.19	171.67	0.25
80040538	Squamous	IIIC1r	1.39	0.38	418.29	0.12	652.81	0.29
80035844			0.15	0.47	0.02	0.36	0.01	0.38
80038243	Squamous	IIIC1r	53.20	0.32	121.49	0.16	1054.64	0.25

(*Continued*)

Table 4 (Continued).

Number	Pathologic types	FIGO staging	LHX2		LHX5		LHX9	
			Gene expression	Promoter methylation level率	Gene expression	Promoter methylation level率	Gene expression	Promoter methylation level率
80035918			1.00	0.40	1.00	0.38	1.00	0.32
80006645	Squamous	IIB	138.99	0.16	327.89	0.12	41.77	0.38
80006791	Squamous	IIIC1r	20.01	0.18	91.54	0.17	1635.49	0.21
80015394	Squamous	IIB	111.77	0.17	38.16	0.18	627.08	0.29
80019860	Squamous	IIIC1r	94.73	0.30	18,871.59	0.06	7045.14	0.04
80021847	Squamous	IIIC1r	52.93	0.36	6269.04	0.09	5199.86	0.05
80024248	Squamous	IIB	3.03	0.39	100.83	0.16	55.44	0.26
80014524	Squamous	IIB	15.62	0.24	69.94	0.18	211.82	0.25
80009713	Squamous	IIB	18.99	0.19	725.03	0.11	224.71	0.22
80033329			1.00	0.41	1.00	0.36		
80019773	Squamous	IIIC1r	2.92	0.35	789.22	0.11	1069.00	0.23
80016920	Squamous cell carcinomas	IVB	20.55	0.19	4983.71	0.06	1089.07	0.23
80019991	Squamous	IIIC1r	1.38	0.39	73.45	0.20	17,499.65	0.02
80010878			1.00	0.41	33.65	0.17	183.04	0.27
80023937	Squamous	IIIC1r	0.06	0.45	796.00	0.10		
80014597	Squamous	IIIC1r	29.61	0.32	60.06	0.22	1986.00	0.19
80008887	Squamous	IIIC1r	0.43	0.46	10,527.30	0.03	208.41	0.25
80008755	Squamous	IIB	1.65	0.36	61.50	0.18	22,868.10	0.14
80014897		IIB	13.74	0.25	1.15	0.32	0.71	0.35
80032097			0.79	0.42	8.48	0.32	3.38	0.29
80024246	Squamous	IIIC1r	0.91	0.42	691.31	0.11	5435.53	0.15

Abbreviations: LHX2, LIM Homeobox 2; LHX2, LIM Homeobox 5; LHX9, LIM Homeobox 9.

Clinical Characteristics of Gene Methylation Level

Clinical Characteristics of Gene Methylation Level

In order to confirm the exact methylation levels in cervical cancer tissues of different patients, the method of BSP-PCR and sequencing was adopted in this study to conduct methylation sequencing on 31 potential sites of each gene. After base confirmation and comparative analysis, LHX2, LHX5 and LHX9 gene methylation levels were determined. Methylation state in target gene promoter in tumor tissue from cervical cancer patients was detected through BSP. As a result, LHX2 gene methylation level increased in cervical cancer, with an average of 38%, the highest of 53%, and the lowest of 16% (Table 4). The LHX2 gene promoter methylation level was generally high among cervical cancer patients. The LHX5 gene methylation level was lower compared with LHX2 gene, with an average of 19.9%, the highest of 42%, and the lowest of only 9%. The methylation level analysis of LHX9 gene showed that the highest methylation rate was 39%, the lowest was 14%, and the average methylation level was 23.7%.

Association of Gene Expression with Stage of Cervical Cancer

The association of gene levels with stage in cervical cancer. The correlation between LHX2, LHX5 and LHX9 gene expression and cervical cancer stage was analyzed. LHX2 gene expression was closely related to stage IIB and IIIC ($P < 0.05$) (Figure 1A); LHX5 gene expression was markedly related to stage IIB and IIIC1R ($P < 0.05$) (Figure 1B); LHX9 was closely related to stage IIB and IIIC ($P < 0.05$) and significantly correlated with stage IIB and IIIC1R ($P < 0.001$) (Figure 1C).

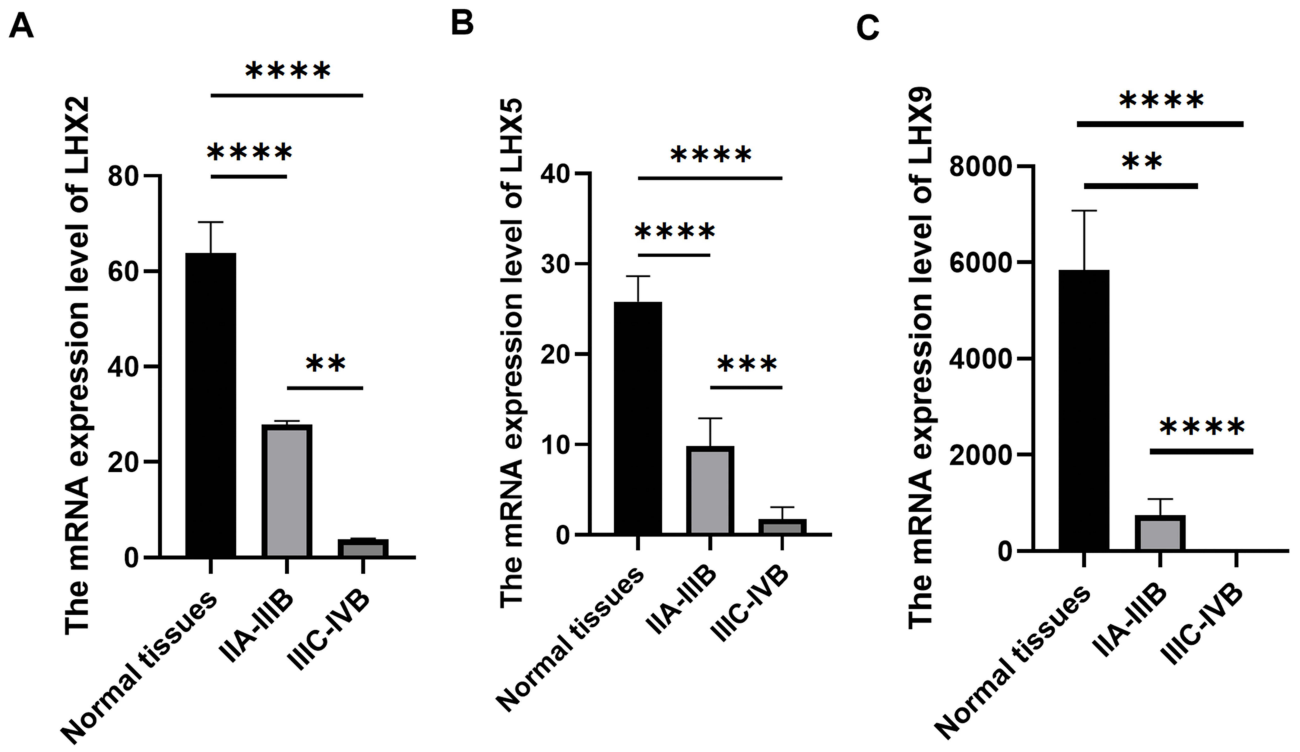

Figure 1 Correlation between LHX2 (**A**), LHX5 (**B**) and LHX9 (**C**) expression and FIGO staging of cervical cancer. **p<0.01, ***p<0.001, and ****p<0.0001 versus normal tissues or IIA-IIIB.

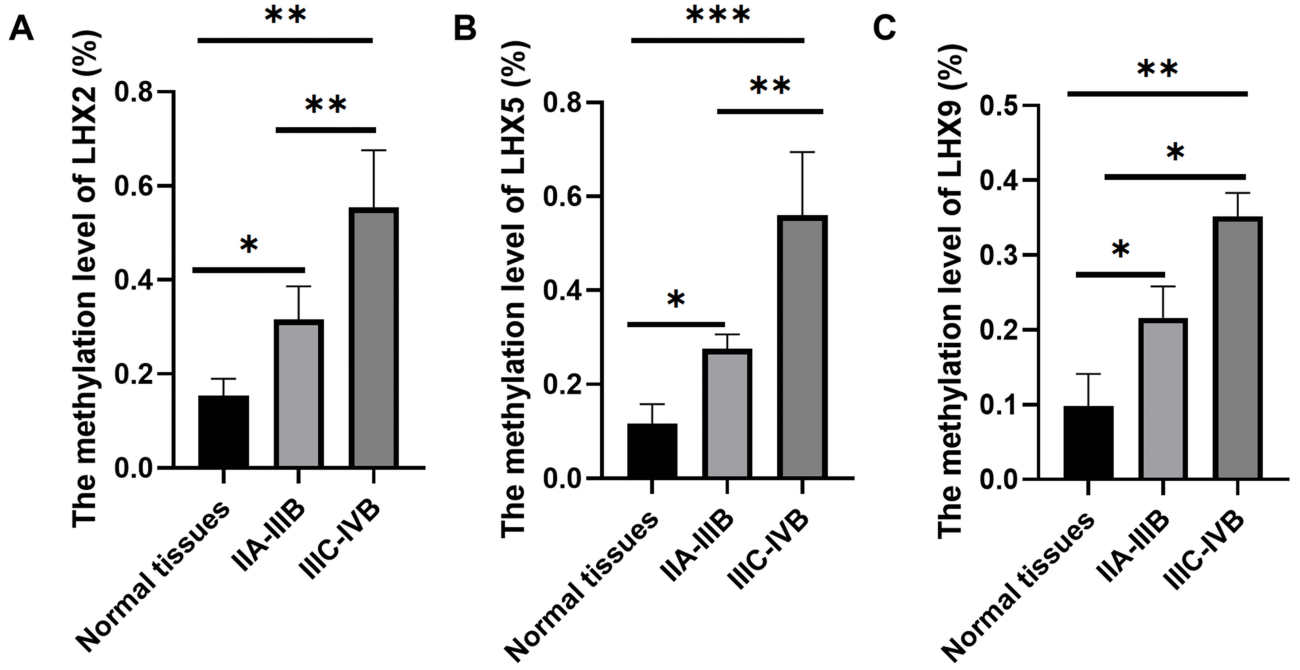

Figure 2 Correlation between LHX2 (**A**), LHX5 (**B**) and LHX9 (**C**) methylation and FIGO staging of cervical cancer. *p<0.05, **p<0.01, and ***p<0.001 versus normal tissues or IIA-IIIB.

The Correlation Between Methylation Levels and Stage in Cervical Cancer

To analyze the correlation between LHX2, LHX5 and LHX9 gene promoter methylation and cervical cancer staging. As a result, the LHX2 gene promoter methylation level was markedly related to stage IIB and IIIC1R ($P < 0.05$)

https://doi.org/10.2147/IJGM.S451841

(Figure 2A); LHX5 gene promoter methylation level was closely related to stage IIB and IIIC1R ($P < 0.05$) (Figure 2B); LHX9 promoter methylation was tightly related to stage IIB and IIIC1R ($P < 0.05$) (Figure 2C).

Methylation Levels in Cervical Cancer Cells

LHX2 and LHX5 and LHX9 Gene Methylation Levels in Cervical Cancer Cells

To identify methylation levels in CpG islands of LHX2, LHX5 and LHX9 genes within SIHA and C33A cells. Meanwhile, to confirm the difference from normal cervical tissue, the study took HCerEpic cells as a control.

It was found that the three genes, LHX2, LHX5 and LHX9, were all highly methylated within cervical cancer cells (Figure 3). The LHX2 gene promoter methylation levels of SIHA cells were 54%, 43%, and 27%, respectively. In contrast, the methylation rates of the three genes in CerEpic cells were 3%, 5% and 2%, respectively. Methylation rates in the C33A cell line were close to SiHA cells, methylation rates in LHX2 LHX5, and in LHX9 gene promoters were 43%, 18% and 29%.

LHX5 and LHX9 Methylation State Within Cervical Cancer Cells Following Radiotherapy

Following radiotherapy, BSP-PCR assay showed that LHX2 and LHX5 methylation rates markedly altered in siHA-2 Gy cells, while LHX2, LHX5, and LHX9 methylation levels decreased to 16%, 21% and 17%, respectively. In C33A - 2 gy cells, LHX2, LHX5 and LHX9 methylation levels dramatically decreased to 8%, 12% and 11%, respectively ($P < 0.05$, Figure 4).

Gene Expression Profiles

Rt-Pcr

Fluorescence qRT-PCR was conducted for detecting target gene level. HCerEpic was also extracted as the control. The quality of the primers of the target gene was detected with the RNA of SIHA and C33A squamous cell carcinoma cells.

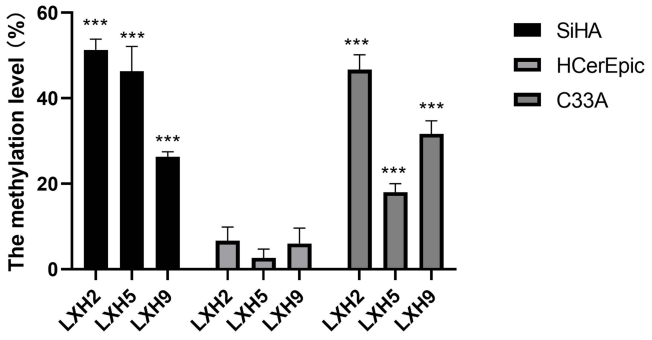

Figure 3 Methylation differences of target genes in different types of cells was compared with that in normal cells. ***$p<0.001$ versus *normal cells*..

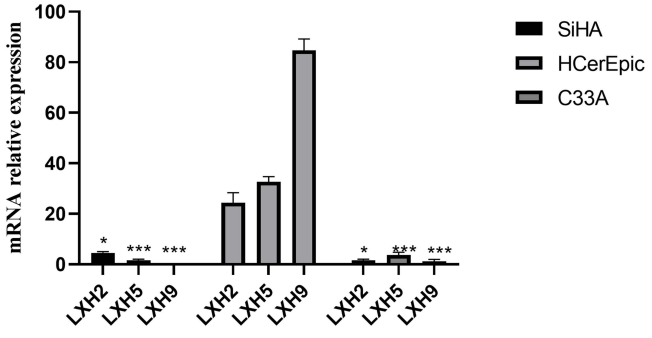

Figure 4 mRNA levels of target genes in different types of cells compared with that in normal cells. *$p<0.05$, ***$p<0.001$ versus *normal cells*..

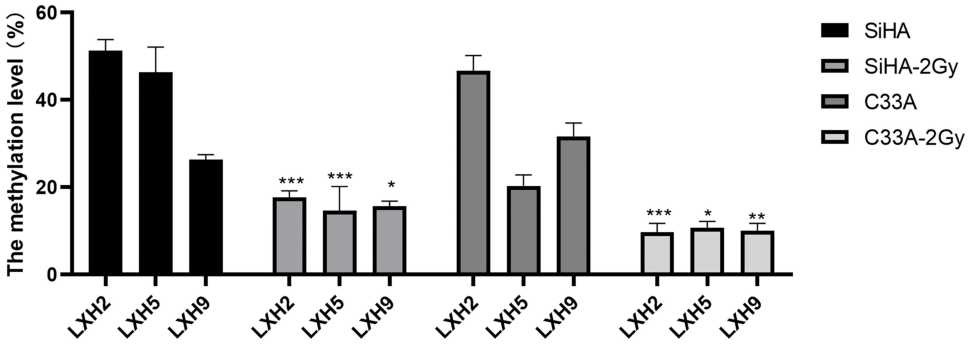

Figure 5 Methylation differences of target genes in different types of cells before and after radiotherapy. *$p<0.05$, **p<0.01,***$p<0.001$ versus *C33A or SiHA*..

Three pairs of primers were found to have a single melting curve, indicating that the amplification product was single and the amplification temperature was 65°C, which met the requirements of quantitative PCR. LHX2, LHX5 and LHX9 gene levels within SIHA and C33A cells and HCerEpic cells were measured.

The three genes had decreased expression in cancer cells relative to HCerEpic cells (Figure 5). The decrease of LHX9 was extremely significant, and the expression of LHX9 was almost undetectable in both cervical cancer cells. LHX2 and LHX5 expression in C33A was 1/15 and 1/30 of those in normal cervical tissue. The expression characteristics of the corresponding LHX2 and LHX5 genes in SIHA cells were 1/20 and 1/8. Following 2Gy ray irradiation, LHX2 and LHX5 gene expression within C33a-2Gy was 3.5 and 4.3 folds of that in the control group (cells with no radiation irradiation). LHX2 and LHX5 expression within SiHA-2Gy cells elevated by 2.3 and 2.5 folds.

Impact of 5-Aza-DC in LHX2, LHX5 and LHX9 Gene Methylation Levels

Following 5-Aza-DC treatment, BSP-PCR assay revealed the markedly altered LHX2 and LHX5 methylation rates within siHA-5-Aza-DC cells. To be specific, the LHX2, LHX5 and LHX9 promoter region methylation rates reduced to 5%, 3% and 4%, respectively. In C33A - 2 gy cells, the LHX2, LHX5 and LHX9 methylation levels significantly decreased to 11%, 16% and 14%, respectively. ($P < 0.05$) (Table 5). Following 5-Aza-DC treatment, methylation rates were different in both cells, with more prominent gene alterations in Siha cells, and lower sensitivity of C33A cells to 5uM 5-Aza-DC.

LHX2 and LHX5 expression within C33A-5-Aza-dC was 3.7 and 4.3 folds of that with no 5-Aza-DC treatment (Figure 6 and Table 6). In addition, LHX2 and LHX5 levels within siHA-2Gy cells increased by 11.3 and 13.9 compared with those without radiation treatment.

Functions of 5-Aza-dC and Radiation in SiHA and C33A Cells

Functions of 5-Aza-dC and Radiation in SiHA and C33A Cell Growth

At present, it has been confirmed that 5-Aza-DC drugs and radiation can reduce the LHX2, LHX5 and LHX9 methylation levels while increasing their mRNA and protein expression. We performed CCK8 assays to detect the proliferation of both cells following 5-Aza-dC and radiotherapy. Because of the toxicity of drugs, the inhibition of cell growth is more significant. There was a 30% difference in growth rate between 24 and 48 hours. At 48 h, the growth rate

Table 5 Effect of 5-Aza-dC Treatment on Methylation Rate of Lhx2, Ihx5 and Lhx9 Genes

	LHX2	LHX5	LHX9
C33A	43±2.3%	29±5.6%	18±2.3%
C33A-5-Aza-dC	11±1.4%	16±2.6%	14±3.4%
siHA	54±4.7%	43±6.3%	27±5.4%
siHA-5-Aza-dC	5±0.4%	3±0.6%	4±0.5%

https://doi.org/10.2147/IJGM.S451841

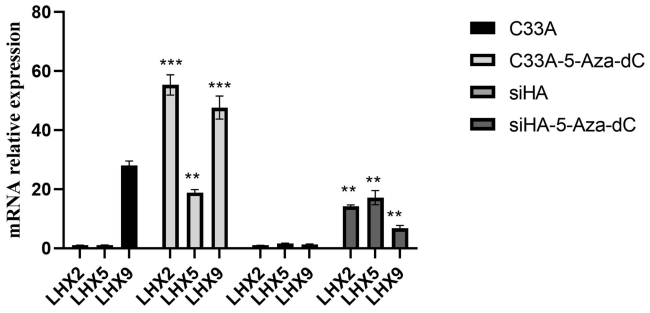

Figure 6 mRNA levels of target genes in different types of cells before and after radiotherapy. **p<0.01,***p<0.001* versus *C33A or SiHA*..

of siHA-5-Aza-dC and Siha-2Gy decreased by 36.3% and 18.9%, respectively. The growth rates of C33A-5-Aza-dC and C33a-2Gy decreased by 14.6% and 21.2%, respectively (Figure 7).

Functions of 5-Aza-dC and Radiation in SiHA and C33A Cell Invasion and Migration

For verifying the role of radiotherapy in cervical cancer cells invasion function, this study adopts 2 Gy dose treatment cell, 24 hours after treatment began to transwell invasion function tests. In siHA cells, siHA-2 gy group after corrosion matrix, complete attack experiment in membrane cells compared to normal siHA, respectively (115 + 10 vs 153 + 5), (16 vs 129 + 153 + 5); Compared with C33a cells, the invasion of experimental permeating cells in the C33a-2Gy group was (146±36. VS.189±14) and (178±25. VS.189±14), separately. The transmembrane cell number significantly declined after 2Gy radiotherapy for both types of cervical squamous cell carcinoma cells ($P < 0.05$) (Table 7).

Similar results were also obtained in the transfer experiment. After SiHA-2Gy group etched the matrix gel, the transferred cells that completed the membrane penetration were (209±33 vs 330±27) compared with the normal SiHA group. Compared with the normal C33A cells, the transmembrane metastatic cells in the C33A-2Gy group were (166±32 vs 264±20). Based on statistical analysis, the transmembrane migratory cell number declined following 2Gy radiation in two cell lines, with a significant difference ($P < 0.05$), suggesting the role of demethylation and radiation in inhibiting cancer cell migration (Table 8).

Discussion

Cervical cancer ranks first and second in terms of its morbidity and mortality among gynecological tumors in China. Radiotherapy remains a mainstream treatment for cervical cancer, which can achieve favorable outcomes particularly for advanced or relapsed cervical cancer patients after surgery.[14] Regardless of the high efficacy of radiotherapy in cervical cancer, this therapeutic modality is associated with certain problems, like decreased radioresistance and radiosensitivity, and shortness of sensitive predictors. DNA methylation, a key epigenetic mode, has a critical effect on genomic structure and function. Methods used to detect DNA methylation are classified as 2 categories: local or genome-wide methylation detection. Thanks to the progress in high-throughput sequencing, research on DNA methylation has developed to genome-wide methylation studies. Traditional methylation detection methods like MSP and BSP are disadvantageous in the few or local site studies, time- and labor-consuming, and low flux. By integrating high-throughput sequencing and

Table 6 mRNA Expression Level of LHX2, LHX5 and LHX9 Genes Treated with 5-Aza-dC and Radiotherapy

	LHX2	LHX5	LHX9
C33A	1.03±0.32	1.06±0.45	178.04±58.35
C33A-5-Aza-dC	55.34±18.83	18.89±5.37	47.65±21.44
siHA	1.01±0.15	1.63±1.75	1.28±1.03
siHA-5-Aza-dC	14.20±2.60	17.16±13.27	6.79±5.25

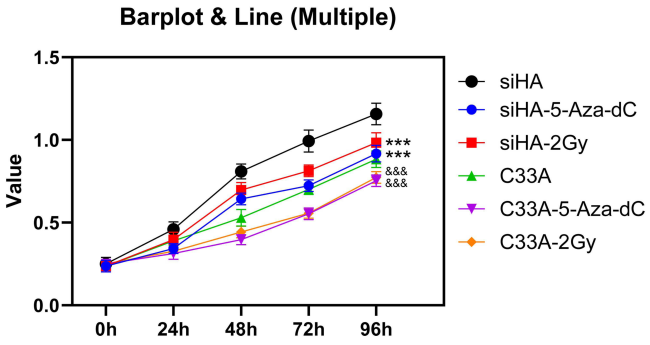

Figure 7 Cell growth curves of different treatments. ***$p<0.001$ versus *SiHa, and* $^{\&\&\&}p<0.001$ versus *C33a.*

BSP, research on DNA methylation targets various sites, covers the whole genome, and concurrently offers methylation rates in various functional regions.[15,16]

In this study, high-throughput sequencing technology was used to conduct whole-genome methylated WGBS sequencing detection and analysis on the cervical cancer self-tissue of three cervical cancer patients before and after radiotherapy. Raw reads averaged 706630178, and average Clean reads were 602534129. The matching rate of high-quality sequencing data before radiotherapy for the three individuals was more than 77%. The matching rate after radiotherapy was more than 75%. The mCG class had the highest proportion, more than 80%, but its proportion was reduced at the methylation site after radiotherapy. MCHG and MCHH loci increased after radiotherapy. In various functional regions of the genome, such as genes, promoters, exons and downs, the four types of mC, mCG, mCHG and mCHH had higher proportions before irradiation than after irradiation. Only MCG decreased by 0.13% after radiation in the promoter region compared with before radiation. The average methylation level of mCG sequence is 58.04% in the promoter region, and the hypermethylation level away from the 5 ‘end is increased. Based on genome-wide methylation analysis, the sites of increased cervical cancer methylation in D and M patients after radiotherapy were significantly more than the sites of decreased cervical cancer methylation, while the opposite was true in patients W. The distribution of DMR on the genome is diverse (promoters, exons, downstream regions of genes and intergene regions, etc.), so the ways of DMR regulation of gene expression are also diverse.

In this experiment, the results of GO enrichment pathway analysis, growth and development, development of cell protrusion and plasma membrane boundary, anatomical structure, cell adhesion and other pathways in the three groups were highly enriched. Based on diverse methylation rates and correlation analysis, we found the genes with markedly decreased methylation rate following radiotherapy, which might be associated with the pathogenic mechanism of cervical

Table 7 Results of Invasion of siHa and C33A Cells by 5-Aza-dC and Radiation

Group	Cell number	Group	Cell number
siHA	153±5	C33A	189±14
SiHA-5-Aza-dC	115±10	C33A-5-Aza-dC	146±36
SiHA-2Gy	129±16	C33A-2Gy	178±25

Table 8 Results of Transfer of siHa and C33A Cells by 5-Aza-dC and Radiation

Group	Cell number	Group	Cell number
siHA	330±27	C33A	264±20
siHA-5-Aza-dC	218±30	C33A-5-Aza-dC	186±22
siHA-2Gy	209±33	C33A-2Gy	166± 32

https://doi.org/10.2147/IJGM.S451841

cancer and the radiotherapy mechanism, like MYC, C10orf11, LHX1, LHX2, LHX5 and LHX9. MYC, a transcription factor, is tightly related to human cancers. C-myc protein is capable of promoting cell cycle progression from GL to S phase, accelerating cell growth and differentiation, and enhancing their apoptosis.[17,18] As discovered by Kubler et al, c-myc was important for cervical lesion occurrence; therefore, it might serve as the biomarker for treating cervical lesions and for later decision-making; moreover, it was identified as an essential biomarker.[18] ANXA8 and C10ORF11 genes have been recognized as potential genes that affect lean body weight variation, and they lay a novel theoretical foundation for sarcopenia.[19] Radiotherapy is effective on D and M patients, but the effect is not that significant among M patients. Meanwhile, the LHX5 and LHX9 genes methylation rates remarkably declined within cervical cancer tissues of D and M patients before and after radiotherapy. Consequently, we paid more attention to the above three genes.

According to our results, the ISL-1 gene protein products were similar to MEC-3[20] and LIN-11[21,22] genes, due to their similar cysteine-rich pattern upstream in the homologous domain. As a result, the pattern that contains similar structures is referred to as LIM. The LIM pattern color-encoded amino acid sequences are referred to as LIM domains, while homeobox genes that contain LIM pattern color are deemed LIM-homeobox genes. Notably, LIM domain also represents the sequence that contains 55 amino acid residues quite conserved in positions histidine and cysteine, and lowly conserved between LIM domains among diverse genes or between diverse LIM domains in one gene. The homeotypic domain downstream of LIM domain shows a high degree of conservation. As the double-zinc finger structure, Lim domain can bind to Zn2+[23,24] since zinc finger proteins are capable of binding to DNA and regulating gene activities. According to in vitro assays on MEC-3 and ISL-1 proteins, the LIM domain modulated homologous domains to DNA within proteins.[25]

LHX family genes are transcription factors essential for signaling, tissue-specific differentiation, cell differentiation, and body size formation in vertebrates and invertebrates.[26] There are 9 LHX members, namely, LHX1-9, discovered from mammals. LHX1 is mostly expressed within the central nervous system; nonetheless, it is verified experimentally to be totally deficient in midbrain and forebrain in mouse head.[27] Furthermore, LHX1 is suggested to act on other gene transcription for regulating cell differentiation in such structures. LHX2 can be expressed in various systems, which has a critical effect. LHX2-/- mice exhibit aberrant hippocampal primordia and cerebral cortex development, with premature stopping of the ocular primordia development.[28] LHX5 exerts a key effect on modulating hippocampal morphological development. In the process of gastrula formation, LHX5 gene can be distributed within the hypothalamus in the mouse diencephalon. LHX9 has a close effect to LHX2 on the nervous system, and it shows specific expression within the mouse gonads. Sperm stem cells from LHX9-/- mice are capable of migration, while somatic stem cells are unable of regeneration, resulting in aberrant gonadal development. Therefore, under normal chromosomal conditions, LHX9 mutation is tightly associated with aberrant gonadal development.[29]

Apart from their function in tissue differentiation, genes of LHX family are tightly related to cancer. LHX3 can serve as the late prognostic biomarker and the metastatic oncogene of hepatocellular carcinoma.[30] LHX4 can suppress tumor development through decreasing alpha-fetoprotein expression in liver cancer.[31] Moreover, LHX2 has been identified as the oncogene for various tumors, and its transgenic expression accelerates vascular maturation, tumor cell migration and invasion, and primary tumor proliferation in breast cancer.[32] LHX2 enhances nasopharyngeal carcinoma proliferation and migration via Wnt pathway,[32–34] and shows abnormal expression within lung cancer and pancreatic duct carcinoma. Also, LHX2 can trigger malignant tumor phenotype of osteosarcoma through activating mTOR pathway and suppressing autophagy.[35] Epigenetic alterations of LHX9 gene facilitate glioma cell migration and invasion.[36]

Conclusion

In this study, genome-wide DNA methylation maps of cervical cancer tissues before and after radiotherapy were successfully constructed. It has been found that LHX5 and LHX9 genes are closely related to cervical cancer. LHX5 and LHX9 have negative effects on cervical cancer. The migration ability of LHX9 silenced cell lines was significantly enhanced after irradiation. Overall, our findings might provide a theoretical basis for the study of the pathogenesis and treatment of cervical cancer. However, our study was conducted with a small sample size of three patients. While this allowed for a detailed analysis of each case, the findings may not be fully representative of the broader population of cervical cancer patients. Larger studies are needed to confirm these results and to generalize our conclusions. The study

focused exclusively on cervical cancer, which limits the applicability of our findings to other types of cancer. Further research is needed to determine if similar methylation patterns and gene expression changes occur in other malignancies. Although WGBS is a powerful tool, it is also resource-intensive and expensive. This may limit its widespread use in clinical settings. Additionally, the bisulfite treatment process can introduce biases that may affect the accuracy of methylation measurements. While we demonstrated the functional effects of gene methylation changes in vitro, in vivo studies are necessary to fully understand the biological and clinical relevance of these findings. Future research should include animal models to validate the effects of LHX gene methylation in a more complex biological context. Our study provides valuable insights into the epigenetic changes associated with radiotherapy in cervical cancer. By highlighting the significant role of LHX genes, we propose new avenues for improving cancer treatment through targeted epigenetic therapies. Future research and clinical trials will be crucial in validating these findings and translating them into effective clinical applications.

Data Sharing Statement

All data can be obtained from the corresponding author upon request.

Ethical Approval

The present work was approved by the Research Ethics Committee at Peking University Cancer Hospital (Inner Mongolia Campus) & Affiliated Cancer Hospital of Inner Mongolia Medical University. All patients provided informed consent.

Consent for Publication

The authors sincerely appreciate the consideration of this work and hope to receive comments from reviewers. The authors authorize your publication.

Author Contributions

Rong Yu, Qin Yu and Jie Shi were in charge of study design, manuscript drafting and statistical analysis. Xue Meng collected and analyzed data. Zhiyuan Deng analyzed data and interpreted results. Jing Suo and Hao Yang designed and revised the study for critical intellectual content. All authors contributed to data analysis, drafting or revising the article, gave final approval of the version to be published, and agree to be accountable for all aspects of the work.

Funding

Inner Mongolia Natural Science Foundation in 2021 (No.2021MS08154).

Disclosure

Our authors claim no competing interests.

References

1. Jemal A, Bray F, Center MM, et al. Global Cancer Statistics. *Ca a Cancer J Clinicians*. 2011;61:69–90. doi:10.3322/caac.20107
2. Wanqing C, Kexin S, Rongshou Z, et al. Cancer incidence and mort ality in China, 2014. *ChinJ Cancer Res*. 2018;30(1):1–12. doi:10.21147/j.issn.1000-9604.2018.01.01
3. Witte T, Plass C, Gerhauser C. Pan-cancer patterns of DNA methylation(J). *Genome Med*. 2014;6(8):66. doi:10.1186/s13073-014-0066-6
4. Auclair G, Weber M. Mechanisms of DNA methylation and demethylation in mammals(J). *Biochimie*. 2012;94(11):2202–2211. doi:10.1016/j.biochi.2012.05.016
5. Feinberg AP, Vogelstein B. Hypomethylation distinguishes genes of some human cancers from their normal counterparts(J). *Nature*. 1983;301(5895):89–92. doi:10.1038/301089a0
6. Krueger F, Andrews SR. Bismark: a flexible aligner and methylation caller for Bisulfite-Seq applications. *Bioinformatics*. 2011;27:1571–1572. doi:10.1093/bioinformatics/btr167
7. Gao HF Identification and identification of abnormal DNA methylation gene promoter and its relationship with mutations in early non-small cell lung cancer [D]. 2017.
8. Kawamatsuki M, Kawamatsuki M, Kawamatsuki M, et al. The role of disulfite in the methylation of gastric cancer.
9. Li M, Li O, Sun J, et al. Relationship between DNA methylation and expression in the promoter region of ZnF772 gene and cervical cancer.

10. Journal of Chinese Academy of Medical Sciences. 2020:164–171.
11. Thu KL, Vucic EA, Kennett JY, et al. Methylated DNA immunoprecipitation. *J Vis Exp :jo VE*. 2009;23:935.
12. Raiche J, Rodriguez-Juarez R, Pogribny I, et al. Sex-and tissue-specific expression of maintenance and de novo DNA methyltransferases upon low dose X-irradiation in mice. *Biochem Biophys Res Commun*. 2004;325(1):39–47. doi:10.1016/j.bbrc.2004.10.002
13. Koturbash I, Baker M, Loree J, et al.. Epigenetic dysregulation underlies radiation-induced transgenerational genome instability in vivo. *Int J Radiat Oncol Biol Phys*. 2006(66):327–330.
14. T GD, GianniniA BG, Di Dio C, et al.. Treatment and Follow-Up of Gynecological Cancers: state of Art and Future Perspectives. *Clin Exp Obstet Gynecol*. 2023;50(8):160. doi:10.31083/j.ceog5008160
15. Pogribny I, Koturbash I, Tryndyak V, et al. Fractionated low-dose radiation exposure leads to accumulation of DNA damage and profound alterations in DNA and histone methylation in the murine thymus. *Mol Cancer Res*. 2005;3:553–561. doi:10.1158/1541-7786.MCR-05-0074
16. Barros-Silva D, J MC, Henrique K, et al.. Profiling DNA Methylation Based on Next Generation Sequencing Approaches: New Insights and Clinical Applications. *Genes*. E429.
17. Jeong M, G GA, Goodell MA. Genome-Wide Analysis of DNA Methylation in Hematopoietic Cells: DNA Methylation Analysis by WGBS. *Methods Mol Biol*. 2017;1633:137–149.
18. Ren R, Horton JR, Zhang X, Blumenthal RM, Cheng X. Detecting and interpreting DNA methylation marks. *Curr. Opin. Struct. Biol.* 2018;53:88–99. doi:10.1016/j.sbi.2018.06.004
19. Kinoshita M, Ikei N, Shin S, et al.. Relationship between human papillomavirus and oncogenes (c—myc,N-myc)amplification in human cervical cancers. *Nihon Gan Chiryo Gakkai Shi*. 25(12):2828.
20. Kubler K, Heinenberg S, Rudlowski C, et al.. c-myc copy number gain is a powerful prognosticator of disease outcome in cervical dysplasia. *Oncotarget*. 6(2):825. doi:10.18632/oncotarget.2706
21. Shu R, Xiao H, Zixuan J. Genome-wide association analysis identifying that genes ANXA8 and C10orf11 are candidate genes for sarcopenia. *J Univer Shang Scie Techn*. 2020;42(3):305–310.
22. Way JC, Chalfie M. mec-3, a homeobox-containing gene that specifies differentiation of the touch receptor neurons in C. elegans. *Cell*. 1988;54 (1):5–16. doi:10.1016/0092-8674(88)90174-2
23. FreydG K, K S, Horvitz HR. Novel cysteine-rich motif and homeodomain in the product of the Caenorhabditis elegans cell lineage gene lin-11. *Nature*. 1990;6269(344):876–879. doi:10.1038/344876a0
24. Lund K, S PJ, Jensen J, et al. Islet expression of Rhombotin and Isl-1 suggests cell type specific exposure of LIM-domain epitopes. *Endocrine*. 1995;3(6):399–408. doi:10.1007/BF02935644
25. Dawid IB, Toyama R, Taira M. LIM domain proteins. *ComptesRendus de l Académie Des Sciences - Series III - Sciences de la Vie*. 1995;318 (3):295–306.
26. Michelsen JW, Schmeichel KL, Winge BDR. The LIM motif defines a specific zinc-binding protein domain. *J Inorganic Biochem*. 1993;90 (10):4404–4408.
27. Xue D, Chalfie YT, Chalfie M. Cooperative Interactions Between the Caenorhabditis elegans Homeoproteins UNC-86 and MEC-3. *Science*. 1993;261:1324–1328. doi:10.1126/science.8103239
28. Kadrmas JL, Beckerle MC. The LIM domain: from the cytoskeleton to the nucleus. *Nat Rev Mol Cell Biol*. 2004;5:920–931. doi:10.1038/nrm1499
29. Birk O, Casiano D, Wassif CA. C. et al. The LIM homeobox gene Lhx9 is essential for mouse gonad formation. *Nature*. 2000;403:909–913. doi:10.1038/35002622
30. Huang B. LHX3 Is an Advanced-stage Prognostic Biomarker and Metastatic Oncogene in Hepatocellular Carcinoma. 31–39.
31. Hung TM, Hu RH, Ho CM, et al.. Downregulation of alpha-fetoprotein expression by LHX4: a critical role in hepatocarcinogenesis. *Carcinogenesis*. 2011;32(12):1815–1823. doi:10.1093/carcin/bgr219
32. Kuzmanov A, Hopfer U, Marti P, Meyer-Schaller N, Yilmaz M, Christofori G. LIM-homeobox gene 2 promotes tumor growth and metastasis by inducing autocrine and paracrine PDGF-B signaling. *Mol Oncol*. 2014;8:401–416. doi:10.1016/j.molonc.2013.12.009
33. Liang TS, Zheng YJ, Wang J, Zhao JY, Yang DK, Liu Z-S. Liu ZS.MicroRNA-506 inhibits tumor growth and metastasis in nasopharyngeal carcinoma through the inactivation oftheWnt/β-catenin signaling pathway by downregulating LHX2. *J Exp Clin Cancer Res*. 2019;38:97. doi:10.1186/s13046-019-1023-4
34. Zhou F, Gou S, Xiong J, Wu H, Wang C, Liu T. Liu T.Oncogenicity of LHX2 in pancreatic ductaladenocarcinoma. *Mol Biol Rep*. 2014;41:8163–8167. doi:10.1007/s11033-014-3716-2
35. Song H, Liu J, Wu X, et al. LHX2 promotes malignancy and inhibits autophagy via mTOR in osteosarcoma and is negatively regulated by miR-129-5p. *Aging*. 2019;11(21):9794–9810. doi:10.18632/aging.102427
36. Vladimirova V, Mikeska T, Waha A, et al.. Aberrant methylation and reduced expression of LHX9 in malignant gliomas of childhood. *Neoplasia*. 2009;11:700–711. doi:10.1593/neo.09406